DOI: 10.17344/acsi.2018.4286 *Acta Chim. Slov.* **2018,** *65,* 630–637

Scientific paper

Plate-Like $Bi_4Ti_3O_{12}$ Particles and their Topochemical Conversion to $SrTiO_3$ Under Hydrothermal Conditions

Alja Čontala,[1,2] Marjeta Maček Kržmanc[1,*] and Danilo Suvorov[1]

[1] *Advanced Materials Department, Jožef Stefan Institute Jamova cesta 39, 1000 Ljubljana, Slovenia*

[2] *International Postgraduate School, Jamova cesta 39, 1000 Ljubljana, Slovenia*

* *Corresponding author: E-mail: marjeta.macek@ijs.si*

Received: 25-05-2018

Abstract

Plate-like $Bi_4Ti_3O_{12}$ particles were synthesized using a one-step, molten-salt method from Bi_2O_3 and TiO_2 nanopowders at 800 °C. The reaction parameters that affect the crystal structure and morphology were identified and systematically investigated. The differences between various $Bi_4Ti_3O_{12}$ plate-like particles were examined in terms of the ferroelectric-to-paraelectric phase transition and the photocatalytic activity for the degradation of Rhodamine B under UV-A light irradiation. The results encouraged us to conduct further testing of the as-prepared $Bi_4Ti_3O_{12}$ plate-like particles as templates for the preparation of plate-like $SrTiO_3$ perovskite particles using a topochemical conversion under hydrothermal conditions. The characteristics of the $Bi_4Ti_3O_{12}$ plates and the reaction parameters for which the $SrTiO_3$ preserved the shape of the initial $Bi_4Ti_3O_{12}$ template particles were determined.

Keywords: $Bi_4Ti_3O_{12}$; Aurivillius layered perovskites; Molten-salt synthesis; Plate-like $Bi_4Ti_3O_{12}$; Template plates; Topochemical conversion

1. Introduction

$Bi_4Ti_3O_{12}$ (BIT) is a member of the Aurivillius-type perovskites that have a layered structure in which pseudo-perovskite $(Bi_2Ti_3O_{10})^{2-}$ units are alternating with $(Bi_2O_2)^{2+}$ layers. As a piezoelectric material with a high Curie temperature of 675 °C, $Bi_4Ti_3O_{12}$ has the potential for use in high-temperature piezoelectric applications.[1,2]

The most common synthesis approaches for the preparation of $Bi_4Ti_3O_{12}$ ceramics and particles are solid-state, molten-salt, hydrothermal and some other methods with lower reaction temperatures, e.g., coprecipitation and sol-gel.[3,4,5] During the preparation of $Bi_4Ti_3O_{12}$ from Bi_2O_3 and TiO_2 in molten salt or by solid-state reaction, secondary phases such as $Bi_{12}TiO_{20}$ or $Bi_2Ti_2O_7$ are commonly formed and must be removed from the product prior to further use due to their detrimental effect on the piezoelectric properties of $Bi_4Ti_3O_{12}$ ceramics.[6–8] Plate-like $Bi_4Ti_3O_{12}$ particles with a side length of around 1 μm and a thickness of 50 nm were formed in molten NaCl/KCl at 800 °C.[9] In contrast to the thickness, the side length of the plates was not uniform, varying from 0.25 μm to 3 μm. He et al. systematically studied the influence of the salt/precursor ratio on the morphology of plate-like $Bi_4Ti_3O_{12}$ particles prepared in molten salt. [10] They observed that the average side length and thickness of the $Bi_4Ti_3O_{12}$ plates decreased with an increase in the amount of salt; however, at high dilutions (molar ratios: NaCl:KCl:$Bi_4Ti_3O_{12}$ ≥32:32:1) the influence of the salt content was no longer significant. These $Bi_4Ti_3O_{12}$ (*00l*)-oriented plates were also proved to be more effective for the photocatalytic degradation of Rhodamine B (RhB) than irregularly shaped $Bi_4Ti_3O_{12}$ particles obtained using the solid-state method.[10] Thickness, surface defects and faceting of the surface are all parameters that influence the photocatalytic activity (PA). $Bi_4Ti_3O_{12}$ particles prepared with the hydrothermal method usually exhibited smaller dimensions and higher aggregation than those prepared in molten salt.[11,12] Therefore, a decision has to be taken regarding the preparation method for the specific application of the material.

In contrast to $MTiO_3$ perovskites (M = Ba, Sr, Pb) with their cubic or tetragonal crystal structures, layered perovskites such as Aurivillius ($Bi_4Ti_3O_{12}$ and $MBi_4Ti_4O_{15}$, where M = Ba, Sr, Pb) and Ruddlesden-Popper ($Sr_3Ti_2O_7$)

have a tendency to grow in an anisotropic shape due to their large crystal anisotropy. [13,14]

These layered perovskites are often used as the structural templates for the preparation of anisotropic $MTiO_3$ perovskites via topochemical conversion.[15–17] The first use of topochemical conversion for the preparation of (100)-oriented $SrTiO_3$ tabular particles was demonstrated by Watari et. al. [18] This conversion was performed by the reaction of a Ruddlesden-Popper $Sr_3Ti_2O_7$ template and TiO_2 in molten KCl between 1000°C and 1200 °C. Saito and Takao were the first to use an Aurivillius $SrBi_4Ti_4O_{15}$ template for the preparation of $SrTiO_3$ (100)-oriented plates with smaller dimensions and a higher aspect ratio (side length 5–10 μm, thickness 0.5 μm).[19] The mechanism of the reaction between $SrCO_3$ and $SrBi_4Ti_4O_{15}$ in the molten salt was further studied by Chang et al., who optimized the reaction conditions to minimize the Bi remains.[15] Under hydrothermal conditions $SrTiO_3$ plate-like particles were produced using other templates such as $H_{1.07}Ti_{1.73}O_4 \cdot nH_2O$ and sheet-like TiO_2 mesocrystals.[20,21] $Bi_4Ti_3O_{12}$ particles were already used for a topochemical conversion to $BaTiO_3$ or $SrTiO_3$ in molten salt.[9,22,23]

Based on our previous work $Bi_4Ti_3O_{12}$ is very appropriate template for preparation of $BaTiO_3$ plate-like particles in the molten salt. [9] To the best of our knowledge, the topochemical conversion from $Bi_4Ti_3O_{12}$ to $BaTiO_3$, $SrTiO_3$ or $CaTiO_3$ particles under hydrothermal conditions has not yet been reported. It is well known that the quality and morphology of the initial precursor particles, in addition to the reaction conditions, greatly influence the particle morphology. In this study we report on the preparation of $Bi_4Ti_3O_{12}$ particles with two morphologies and their topochemical transformation to $SrTiO_3$ under hydrothermal conditions.

2. Methods

2. 1. Experimental

$Bi_4Ti_3O_{12}$ plates were synthesized using the molten-salt method. The salts KCl (Sigma-Aldrich, ≥ 99.0%) and NaCl (Merck, ≥ 99.7%) were weighed in a 1:1 molar ratio, ground and mixed well in a mortar to achieve a homogeneous mixture. Next, an appropriate amount of Bi_2O_3 nanopowder (99.9% Alfa Aesar) and TiO_2 nanopowder (P25, Degussa) were weighed, added to the salt mixture and mixed well again. A homogeneous mixture of powder was then transferred to the Al_2O_3 crucible, covered and placed in the furnace. The heating rate was 10 °C/min until the temperature reached 800 °C. The morphology and crystal structure for the $Bi_4Ti_3O_{12}$ obtained under different reaction conditions were investigated in order to determine the best reaction conditions for the preparation of well-developed, plate-like $Bi_4Ti_3O_{12}$ particles with a narrow size distribution. The influence of various reaction conditions such as time (20 minutes and 2 hours), Bi:Ti molar ratio (1.33, 2.0 and 2.67), NaCl:KCl:$Bi_4Ti_3O_{12}$ molar ratio (50:50:1 or 25:25:1) and cooling rate (5 °C/min, 10 °C/min and natural cooling) were examined. In the case of natural cooling, the heating system was turned off after the reaction was performed, and the product was left in the furnace until the furnace reached room temperature. Natural cooling means uncontrolled cooling in a furnace by natural convection, conduction and radiation to room temperature. It was demonstrated that the cooling time from 800 °C to the eutectic temperature of 650 °C in the case of natural cooling was 8 minutes, while for cooling rates of 10 °C/min and 5 °C/min, the cooling times were 15 and 30 minutes, respectively. In this temperature range, where the particle growth still took place, the natural cooling was the fastest. Below 650 °C, the diffusion is expected to be too slow and thus the growth of the particles is negligible. For comparison, $Bi_4Ti_3O_{12}$ was also synthesized under selected conditions (Bi:Ti = 1.33, 800 °C 2 h, natural cooling) using anatase TiO_2 (Sachtleben Pigments Oy, HOMBITAN AFDC 001517011, 99%) μm-sized powder instead of the P25 nanopowder.

After the reaction, the product powders were washed with deionized water by suction filtration in order to remove the salt. Afterwards, they were also washed with 2-M HNO_3 (soaking time 10 minutes) in order to remove the secondary phases and finally with deionized water again (until pH = 7). The product powders were freeze-dried.

In the second part of the study, $Bi_4Ti_3O_{12}$ template plates were tested for the topochemical conversion to $SrTiO_3$ under hydrothermal conditions. For this reaction $SrCl_2 \times 6H_2O$ (Sigma Aldrich, ≥ 99%) was added to the $Bi_4Ti_3O_{12}$ in the molar ratio Sr:Ti = 3. The reaction was performed under hydrothermal conditions in 4-M NaOH (Merck, 99%) with stirring at 200 °C for 12 hours. The product was cooled naturally and washed with deionized H_2O, 1-M HNO_3 and once again with deionized H_2O. The product was freeze-dried.

2. 2. Characterization

The crystal structure was characterized with X-ray powder diffraction (Bruker AXS D4 Endeavor) using Cu–K_α radiation (1.5406 Å). For an estimation of the preferential orientation, a few drops of suspension of the particles in iso-propanol were deposited on a Si single crystal and left for the alcohol to evaporate. The morphology and size of the prepared particles were studied by field-emission scanning electron microscopy (FE-SEM, JSM 7600 F, JEOL). The specific surface area was measured using the BET method with nitrogen adsorption (Gemini 2370 V5.00).

For the PA of the $Bi_4Ti_3O_{12}$ particles, the decomposition of RhB was measured in UV-A light. The concentration of the sample, mixed with RhB and exposed to UV-A light, was 0.2 mg/ml, and the concentration of the RhB was 10 mg/l. Prior to irradiation, the solution was sonicated for

1 minute (pulse:pause was 2:1 seconds) at 80% and afterwards it was stirred in the dark at 500 rpm for 30 minutes. Samples were taken before irradiation and after 1 h, 2 h, 3 h, 4 h and 24 hours of irradiation with UV-A light. The powder was removed after centrifugation. The absorbance was measured at λ = 554 nm using a Synergy Micro Plate Reader (BIOTEK). Control reactions in the dark for RhB with the sample and a parallel reaction for pure RhB were also performed. Differential scanning calorimetry (DSC) measurements were made on a Jupiter 449 simultaneous thermal analysis (STA) instrument (Netzsch, Selb, Germany). The measurements were made with a heating rate of 20 °C/min in an Ar/O_2 (40/20) atmosphere using a TG/DSC-cp sample holder and platinum crucibles. The temperature and enthalpy calibrations of the STA instrument were made with $BaCO_3$, CsCl, K_2CrO_4, $KClO_4$ and $RbNO_3$ standards.

3. Results and Discussion

3. 1. Influence of the Reaction Conditions on the Morphology and Crystal Structure

$Bi_4Ti_3O_{12}$ was formed in the molten salt by dissolution-precipitation. This means that Bi_2O_3 and TiO_2 firstly dissolved in the molten salt and then $Bi_4Ti_3O_{12}$ plates precipitated at a high degree of supersaturation. Further growth of the plates occurred by Ostwald ripening. Therefore, the particle size could be tailored with the duration of the reaction. Longer and shorter times were selected for the preparation of larger (μm-sized) and smaller (sub-μm-sized) $Bi_4Ti_3O_{12}$ plates, respectively.[9] In particular, sub-μm- and nano-sized anisotropic particles of ferroelectrics ($Bi_4Ti_3O_{12}$ and $BaTiO_3$) have recently become of great scientific and technological interest due to their unique shape- and size-dependent functional properties with reduced sub-μm-size dimensions. At first, the phase composition and morphology of the $Bi_4Ti_3O_{12}$ particles obtained at 800 °C after 2 hours in the first experiment (BIT1) and 20 minutes in the second experiment (BIT2) were examined and compared (Fig. 1, Table 1). In both of these cases the reaction was performed with surplus Bi_2O_3 (Bi:Ti = 2.67, stoichiometric Bi:Ti = 1.33). The Bi_2O_3 was added in excess in order to provide a high concentration of Bi^{3+} for the formation of $Bi_4Ti_3O_{12}$ plates. In the case of a shorter synthesis time (20 minutes), the $Bi_4Ti_3O_{12}$ plates exhibited a smaller average side length as well as a reduced thickness compared to the plates obtained after a longer synthesis time (2 hours), when the particles had more time available for Ostwald-ripening growth. In both cases the XRD analyses showed that a significant amount of $Bi_{12}TiO_{20}$ secondary phase (PDF #034-0097) was present (Fig. 2, XRD pattern A) in addition to the $Bi_4Ti_3O_{12}$ (PDF #035-0795). The formation of $Bi_{12}TiO_{20}$ was a consequence of excess Bi_2O_3 in the reaction mixture. During washing with 2-M HNO_3 the $Bi_{12}TiO_{20}$ was dissolved and monoclinic $Bi_4Ti_3O_{12}$ became the only phase in both cases. Reaction conditions for the described $Bi_4Ti_3O_{12}$ (BIT1 and BIT2) and for the $Bi_4Ti_3O_{12}$ prepared under other conditions are presented in Table 1. Bi:Ti and NaCl:KCl:$Bi_4Ti_3O_{12}$ are molar ratios.

In the next step the molar ratio of bismuth to titanium (denoted as Bi:Ti in Table 1) was studied. We selected three values of Bi:Ti: 2.67, 2.0 and 1.33 (stoichiometric) for BIT3, BIT4 and BIT5, respectively. In the experiment using a ratio of 1.33 the plates had a more defined shape and a narrower size distribution (Fig. 1C) than in the other two cases and $Bi_4Ti_3O_{12}$ was the main phase, observed by XRD after the synthesis. In the other two cases, washing with HNO_3 was necessary to remove the secondary $Bi_{12}TiO_{20}$ phase.

The influence of the amount of salt on the morphology and crystal structure was also investigated. In accordance with the literature[10] we used a 50:50:1 molar ratio (BIT6) of KCl:NaCl:$Bi_4Ti_3O_{12}$. However, when the ratio was reduced to 25:25:1 (BIT5) the size distribution of the product particles became more uniform. With a smaller amount of salt, the diffusion distance of the reactant particles is smaller; therefore, the reaction occurs faster and more uniformly. Powder XRD patterns confirmed the dominance of the monoclinic $Bi_4Ti_3O_{12}$ phase (PDF #035-0795) for both products.

Table 1: Reaction conditions of BIT1-BIT9 for the investigation of the influence of the reaction parameters on the morphology and crystal structure of $Bi_4Ti_3O_{12}$

Sample	TiO_2	Bi:Ti	NaCl:KCl:$Bi_4Ti_3O_{12}$	T (°C)	Time	Heating	Cooling
BIT1	P25	2.67	50:50:1	800	2 h	10 °/min	10 °/min
BIT2	P25	2.67	50:50:1	800	20 min	10 °/min	10 °/min
BIT3	P25	2.67	25:25:1	800	2 h	10 °/min	10 °/min
BIT4	P25	2.0	25:25:1	800	2 h	10 °/min	10 °/min
BIT5	P25	1.33	25:25:1	800	2 h	10 °/min	10 °/min
BIT6	P25	1.33	50:50:1	800	2 h	10 °/min	10 °/min
BIT7	P25	1.33	25:25:1	800	2 h	10 °/min	5 °/min
BIT8	P25	1.33	25:25:1	800	2 h	10 °/min	natural
BIT9	anatase	1.33	25:25:1	800	2 h	10 °/min	natural

Cooling rates of 10 °C/min (BIT6), 5 °C/min (BIT7) and natural cooling (BIT8-Fig. 2D) were also compared. Based on SEM observations we concluded that there is no significant difference in the morphology when the cooling rates were 10 °C/min, 5 °C/min or natural cooling.

The most differing BIT products (BIT2 and BIT8) were selected for further analysis. SEM micrographs and XRD patterns for those plate-like $Bi_4Ti_3O_{12}$ samples are shown in Figures 1 and 2, respectively. The higher degree of aggregation of BIT2 compared to BIT8 is evident from the SEM micrographs as well as from the XRD patterns of the $Bi_4Ti_3O_{12}$ particles deposited on the Si single crystal (Figure 2, XRD patterns C and D). Due to the random orientation of the plate-like $Bi_4Ti_3O_{12}$ particles in the aggre-

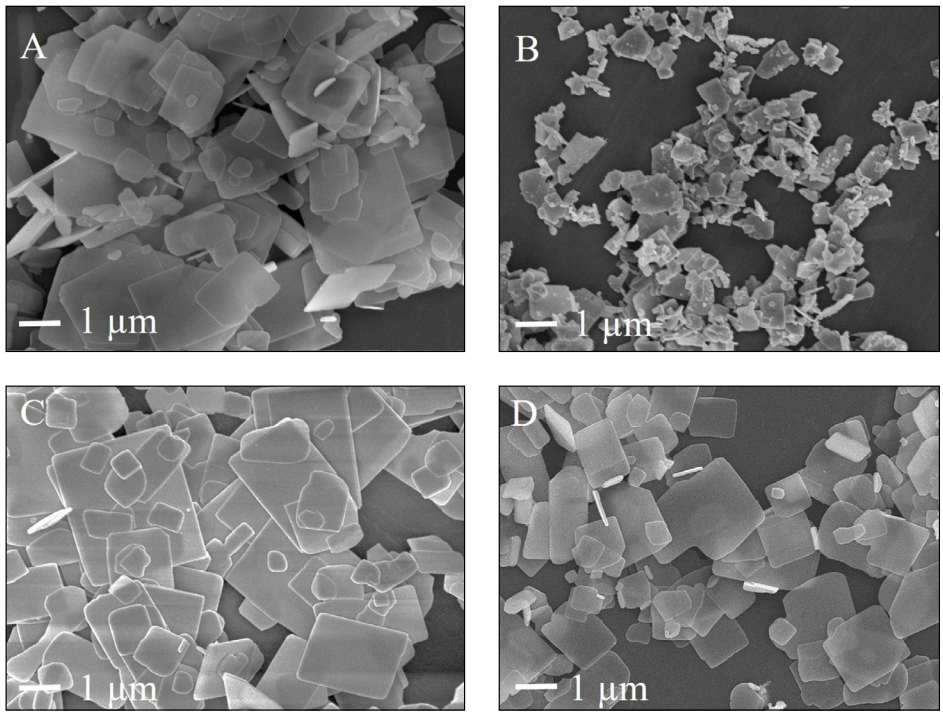

Figure 1: SEM micrographs of the $Bi_4Ti_3O_{12}$ plates that were synthesized at 800 °C for 20 min (B-BIT2) and for 2h (A-BIT1, C-BIT5, D-BIT8). Other synthesis details are shown in Table 1.

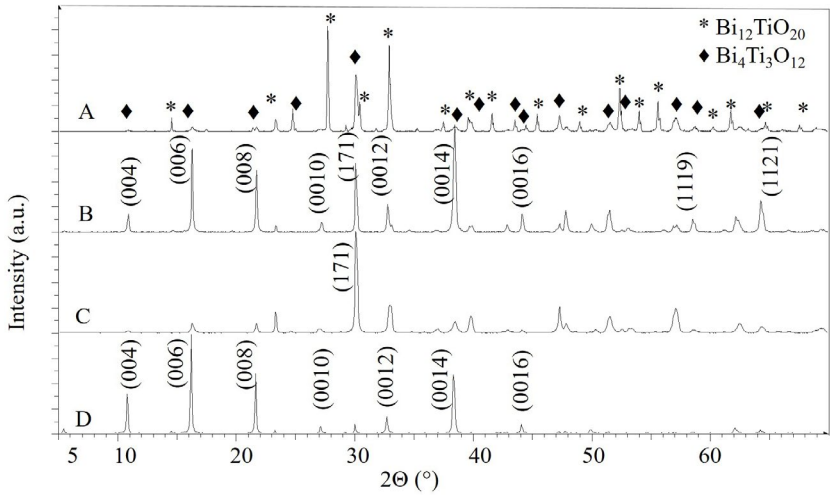

Figure 2: XRD patterns of $Bi_4Ti_3O_{12}$ plates prepared at 800 °C *for 20 min (*patterns A and C for BIT2) and for 2 h (patterns B and D for BIT8). The A and B patterns represent the XRD patterns of $Bi_4Ti_3O_{12}$ powders washed only by water in order to determine possible secondary phases. The XRD patterns C (for BIT2) and D (for BIT8) were obtained from $Bi_4Ti_3O_{12}$ plates that were cast on the Si single crystal. The $Bi_4Ti_3O_{12}$ plates prepared for examination of their average preferential orientation in these two patterns were washed with 2-M HNO_3 to ensure a single-phase product. In the XRD pattern A, ♦ and * denote the $Bi_4Ti_3O_{12}$ and $Bi_{12}TiO_{20}$ phases, respectively. The hkl indexation is given for $Bi_4Ti_3O_{12}$.

gates of BIT2 sample, the relative intensities of the (*00l*)/(*117*) planes (*l* = even number) were considerably lower in comparison to those of the larger $Bi_4Ti_3O_{12}$ (BIT8) plates, which oriented during deposition on a Si single crystal in a way that the (*00l*) planes were parallel to the substrate. Based on this we can infer that 1–2-μm-sized $Bi_4Ti_3O_{12}$ plates exhibited a high (*00l*) preferential orientation (Figure 2, XRD pattern D).

Finally, $Bi_4Ti_3O_{12}$ was also prepared from μm-sized anatase TiO_2 particles (BIT9) instead of P25 TiO_2 nanopowder, but under the same reaction conditions as for the BIT8. As expected, the plates were less uniform in size. The majority of the plates were much smaller (approx. 100 nm) and the rest were between 1 and 2 microns. This non-uniform particle size distribution was most probably a consequence of the larger anatase particles, which dissolved more slowly and unevenly than the P25 nanoparticles. Also in this case, the XRD pattern confirmed that monoclinic $Bi_4Ti_3O_{12}$ was the main phase.

For smaller and larger $Bi_4Ti_3O_{12}$ plates (BIT2 and BIT8) the specific surface area (BET), the photocatalytic activity (PA) and the DSC measurements were performed in order to confirm the significant difference in size and the specific surface area. The BET results were in agreement with the SEM observations. The specific surface area was larger for BIT2 than for BIT8 (Table 2), which is in accordance with the SEM observation and confirmed that the BIT2 particles were smaller and consequently the specific surface area was larger than for BIT8.

Since it is well known that PA is influenced by many factors such as surface defects, particle size, morphology, crystallinity and band gap, we decided to test both types of plates in terms of their capability to degrade organic dye (RhB) under UV-A radiation. A high concentration of defects is not beneficial, neither for the photocatalysis nor for the epitaxial growth of a new phase on the template. Nevertheless, the acceptable level of defects is different for both processes. For photocatalysis, some defects are advantageous when they introduce intermediate surface states that narrow the band gap. In general, a high density of defects, which act as recombination centers for photo-induced electrons and holes, lowered the PA. The photodegradation of RhB in BIT2 was 88% and in BIT8 it was 65% after 4 hours of irradiation with UV-A light. This confirmed our expectations that the PA of BIT2 is larger than that of BIT8. The larger PA of BIT2 can also be ascribed to smaller particles with a higher specific surface area, which provide more active sites for the photocatalytic reaction.

For the DSC measurements both samples (BIT2 and BIT8) were first washed with 2-M HNO_3 to ensure single-phase $Bi_4Ti_3O_{12}$. The DSC measurements revealed a very similar DSC peak temperature (T_c) for the ferroelectric-to-paraelectric phase transition for both types of $Bi_4Ti_3O_{12}$ plates (643.6 °C for BIT2 and 642.9 °C for BIT8) (Fig. 3). However, the absolute values of the phase-transition enthalpies ($|\Delta H_{FET}|$) of the two samples differ significantly. The measured $|\Delta H_{FET}|$ for BIT2 and BIT8 were 1.457 J/g and 4.555 J/g, respectively (Fig. 3, Table 2). The decrease of the phase-transition enthalpy with a decrease in the particle size was already observed for other ferroelectric particles ($BaTiO_3$).[24] Taking into account that the enthalpy of the phase transition is proportional to the polarization (P) ($\Delta H_{FET} = 2\,\pi P^2\,T_c\,/C$ (Eq. 1), where C is the Curie-Weiss constant) the decrease of $|\Delta H_{FET}|$ could be explained by the decrease of P. It is also known that the phase-transition enthalpy is related to the domain structure.[24,25] The larger $|\Delta H_{FET}|$ of BIT8 could correlate with larger particles and be expected to exhibit a multi-domain structure. Due to the domain clamping the enthalpy of the phase transition was higher for larger particles compared to the single-domain smaller particles. In addition, with a decrease of the particle size, the ratio between the disordered surface and the ordered bulk is increasing, which additionally causes a destruction of the polar state.[24]

3. 2. $Bi_4Ti_3O_{12}$ Plates as a Template for Topochemical Conversion to $SrTiO_3$

Due to the pseudo-perovskite units the $Bi_4Ti_3O_{12}$ plates are regarded as a suitable template for the preparation of $MTiO_3$ perovskite plates via topochemical conversion. It was already shown that the transformation from $Bi_4Ti_3O_{12}$ to $BaTiO_3$ is possible in the molten salt.[9] There is great interest in whether this kind of conversion is also

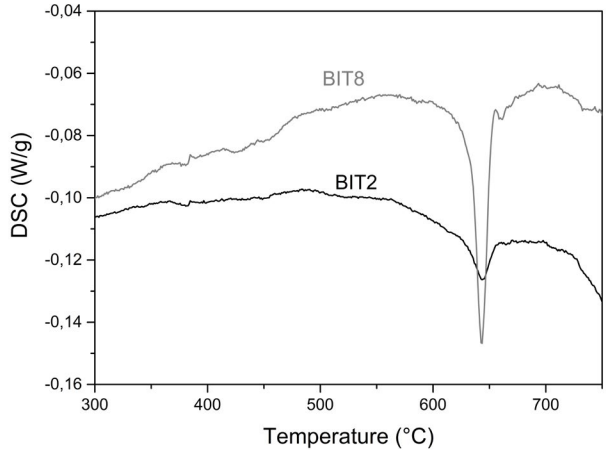

Figure 3: DSC curves of *$Bi_4Ti_3O_{12}$ plates during heating for BIT2 and BIT8 sample.*

Table 2: Results for BET, DSC and PA measurements of BIT2 and BIT8

Sample	BET (m^2/g)	T_c (°C)	(J/g)	$PA_{4\ hours}$
BIT2	2.9075	643.6	1.457	88.6%
BIT8	0.4855	642.9	4.555	65.0%

possible under hydrothermal conditions. Kalyani et al. studied the hydrothermal crystallization of $SrTiO_3$ on anatase nanowires and proved that the formation of $SrTiO_3$ was driven by the topochemical reaction,[26] since the formed $SrTiO_3$ mesocrystals retain the wire-like shape of the initial anatase particles. To the best of our knowledge there are no literature reports about the topochemical conversion of $Bi_4Ti_3O_{12}$ to $MTiO_3$ perovskites under hydrothermal conditions. In the present study we firstly aimed to examine whether under these conditions $Bi_4Ti_3O_{12}$ plates are an appropriate template for the preparation of $SrTiO_3$ plates and secondly we wanted to verify how differently sized $Bi_4Ti_3O_{12}$ template plates (sub-μm- and above-μm-sized) influenced the final morphology of the $SrTiO_3$ particles. From the standpoint of advanced development and the improvement of applications and electronic devices, controlling the shape and size of particles can lead to new or combined and improved properties of existing materials. The miniaturization of electronic devices is also of great interest in nanotechnology; however, it is already well known that materials lose some of their functional properties (i.e., ferroelectricity) below certain small dimensions. Additionally, it is easier to observe the growth of $SrTiO_3$ on larger plates. For this reason we decided to study the formation of $SrTiO_3$ from two types of $Bi_4Ti_3O_{12}$: smaller, sub-μm-sized, $Bi_4Ti_3O_{12}$, plate-like particles with a broad particle size distribution (BIT2) and larger, 1–2-μm-large and well-defined $Bi_4Ti_3O_{12}$ plates (BIT8). The XRD examination of the reaction products in both cases confirmed the formation of $SrTiO_3$ (PDF #035-0734) from the $Bi_4Ti_3O_{12}$ plates under alkaline (4-M NaOH) hydrothermal conditions at 200 °C for 12 hours (Fig. 4, XRD pattern A). The smaller $Bi_4Ti_3O_{12}$ template particles (BIT2) that were very non-uniform in size, consequently resulted in a non-ideal morphology of the $SrTiO_3$ particles. This means that the as-prepared $SrTiO_3$ particles differed in their shape and size. The cube-like particles prevailed, but some of them also exhibited a preferable plate-like shape (Fig. 5A). In contrast, the $SrTiO_3$ particles prepared from larger $Bi_4Ti_3O_{12}$ template plates (BIT8) preserved the shape of the template. The XRD revealed that *(00l)*-oriented $Bi_4Ti_3O_{12}$ plates transformed into *(h00)*-oriented $SrTiO_3$ plates (Fig. 4, XRD pattern B). However, the morphology of the $SrTiO_3$ plates was still not perfect. The particles varied in their size, which was most probably the consequence of the non-uniform size distribution of the initial $Bi_4Ti_3O_{12}$ plates. Figure 5B demonstrates that there were small holes present in some of those $SrTiO_3$ plates. These holes were also observed when the $SrTiO_3$ plates were washed only with water after the synthesis. Therefore, the holes were not formed during HNO_3-washing, although HNO_3 is a strong acid and could cause the leaching of Sr and the remains of Bi from the plates. Additionally, the holes were not formed due to the HNO_3 washing of the $Bi_4Ti_3O_{12}$ template plates, because the holes were also present in the $SrTiO_3$ plates, which were prepared from the water-washed $Bi_4Ti_3O_{12}$ plates. Thus, the holes were not a consequence of the etching effect of the HNO_3, although it is known that chemical etching can cause square-shaped holes in $Bi_4Ti_3O_{12}$ grains.[27] These holes were either the consequence of the defective surface of the $Bi_4Ti_3O_{12}$ plates or originated from the lattice mismatch between the pseudo-perovskite layer of the template and the $SrTiO_3$ plates. In addition, the removal of the $(Bi_2O_2)^{2+}$ layer during the conversion could also cause exfoliation, the result of which could be those holes. An examination of the morphology of the $SrTiO_3$ particles prepared from the different $Bi_4Ti_3O_{12}$ template plates revealed that the completeness of the $SrTiO_3$ plates strongly depended on both the quality of the $Bi_4Ti_3O_{12}$ template plates and the reaction conditions. For example, the worst preservation of the initial $Bi_4Ti_3O_{12}$ template shape during the conversion to $SrTiO_3$ was observed for the $Bi_4Ti_3O_{12}$ plates that were prepared from the large, μm-sized, TiO_2 anatase particles. With this study we confirmed that the μm-sized $Bi_4Ti_3O_{12}$ plate-like particles with a rather uniform particle size distribution (i.e. BIT8) can be used as a template for the topochemical transformation to plate-like $SrTiO_3$ particles with a *(h00)* preferential orientation.

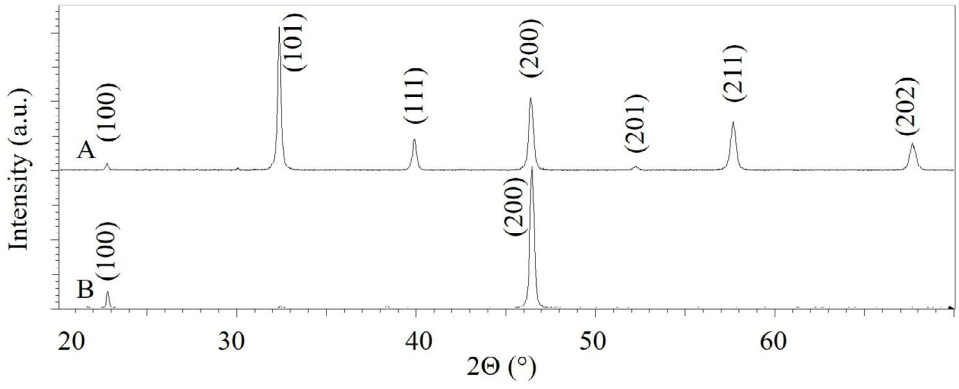

Figure 4: XRD patterns of $SrTiO_3$ powder prepared from BIT8 (pattern A) and $SrTiO_3$ plates cast on the Si single crystal (pattern B). XRD pattern of the $SrTiO_3$ plates deposited on the Si single crystal revealed that their preferential orientation was (100).

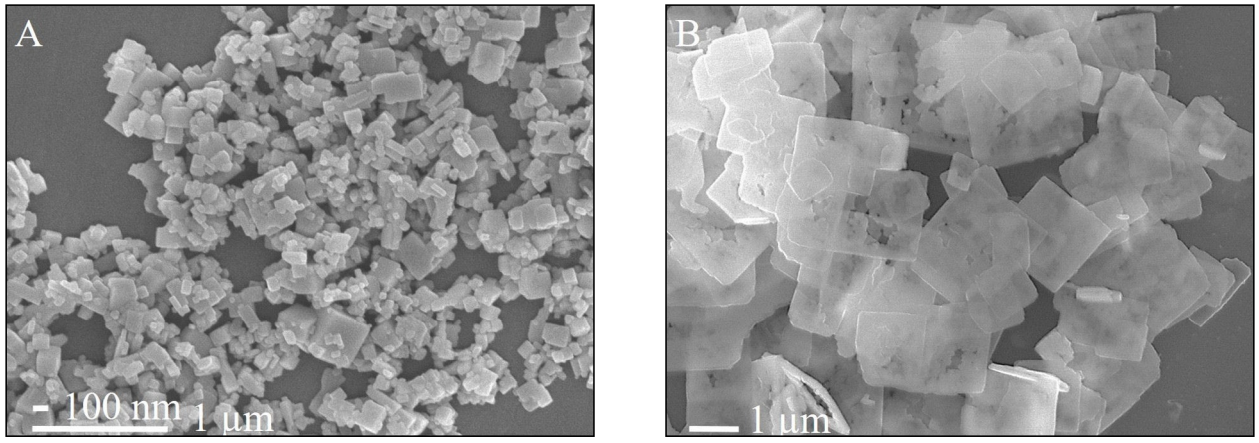

Figure 5: SEM micrographs of $SrTiO_3$ particles obtained from the topochemical conversion of different $Bi_4Ti_3O_{12}$ plate-like particles under the same hydrothermal reaction conditions (Sr:Ti molar ratio 3:1, 4-M NaOH, 200 °C for 12 hours). The $SrTiO_3$ particles A were prepared from the BIT2 template and the $SrTiO_3$ particles B were prepared from the BIT8 template.

4. Conclusions

In the first part of this research the influence of molten-salt synthesis conditions on the morphology of $Bi_4Ti_3O_{12}$ plate-like particles was studied. The most appropriate conditions for the growth of µm-sized $Bi_4Ti_3O_{12}$ plates with a uniform size distribution are as follows: Bi:Ti molar ratio = 1.33 (stoichiometric), molar ratio of NaCl:KCl:$Bi_4Ti_3O_{12}$ = 25:25:1 and 2-hour reaction time at 800 °C.

In the second part of the study we proved that the as-prepared $Bi_4Ti_3O_{12}$ plates are an appropriate template for the preparation of plate-like (*h00*)-oriented $SrTiO_3$ plates using a topochemical conversion under hydrothermal conditions. We also confirmed that the type of TiO_2 precursor (P25 or anatase used for $Bi_4Ti_3O_{12}$ synthesis) has a great influence on the morphology of the formed $Bi_4Ti_3O_{12}$ plate-like particles, which, when transformed to $SrTiO_3$ under hydrothermal conditions, result in even more diverse morphologies. The photodegradation of RhB, BET and DSC measurements confirmed the difference between the used templates. These results also support the choice of template for the topochemical conversion of $Bi_4Ti_3O_{12}$ to $SrTiO_3$ under hydrothermal conditions.

5. Acknowledgement

The authors acknowledge the project J2-6753 and the M-era.Net project 3184 HarvEnPiez, which were financially supported by the Slovenian Research Agency and the Ministry of Higher Education Science and Technology, respectively. Alja Čontala is grateful to the Slovenian Research Agency for the financial support of her PhD study. The authors would like to thank Martyna Durko for performing the photocatalytic measurements.

6. References

1. Z. Lazarević, B. D. Stojanović, J. A. Varela, *Sci Sinter*. **2005**, *37*, 199–216. **DOI:**10.2298/SOS0503199L
2. Z. Lazarević, N. Rom, M. Todorović, B. D. Stojanović, *Sci Sinter*. **2007**, *39*, 177–184. **DOI:**10.2298/SOS0702177L
3. F. Zhang, T. Karaki, M. Adachi, *Jpn J Appl Phys*. **2006**, 45, 7385–7388. **DOI:**10.1143/JJAP.45.7385
4. M. Villegas, C. Moure, J. F. Fernandez, P. Duran, *J Mater Sci*. **1996**, *31*, 949–955. **DOI:**10.1007/BF00352895
5. Y. G. Zhang, H. W. Zheng, J. X. Zhang, et al, *Mater Lett*. **2014**, *125*, 25–27. **DOI:**10.1016/j.matlet.2014.03.146
6. M. G. Navarro-Rojero, J. J. Romero, F. Rubio-Marcos, J. F. Fernandez, *Ceram Int*. **2010**, *36*, 1319–1325. **DOI:** 10.1016/j.ceramint.2009.12.023
7. M. Villegas, A. C. Caballero, C. Moure, P. Duran, J. F. Fernandez JF, *J Am Ceram Soc*. **1999**, *82*, 2411–2416. **DOI:**10.1111/j.1151-2916.1999.tb02098.x
8. T. Zaremba, *J Therm Anal Calorim*. **2008**, *93*, 829–832. **DOI:**10.1007/s10973-008-9330-6
9. M. M. Kržmanc, B. Jančar, H. Uršič, M. Tramšek, D. Suvorov, *Cryst Growth Des*. **2017**, *17*, 3210–3220. **DOI:**10.1021/acs.cgd.7b00164
10. H. He, J. Yin, Y. Li, et al, *Appl Catal B Environ*. **2014**, *156–157*, 35–43. **DOI:**10.1016/j.apcatb.2014.03.003
11. Z. Chen, Y. Yu, J. Hu, A. Shui, X. He, *J Ceram Soc Japan*. **2009**, *117*, 264–267. **DOI:**10.2109/jcersj2.117.264
12. Q. Yang, Y. Li, Q. Yin, P. Wang, Y. B. Cheng, *J Eur Ceram Soc*. **2003**, *23*, 161–166. **DOI:**10.1016/S0955-2219(02)00087-0
13. T. Takeuchi, T. Tani, *J Ceram Soc Japan*. 2002, 110, 232–236. **DOI:**10.2109/jcersj.110.232
14. R.E. Schaak, T.E. Mallouk, *Chem Mater*. 2002, 14, 1455–1471. **DOI:**10.1021/cm010689m
15. Y. Chang, H. Ning, J. Wu, et al, *Inorg Chem*. **2014**, *53*, 11060–11067. **DOI:**10.1021/ic501604c
16. S. F. Poterala, Y. Chang, T, Clark, R. J. Meyer, G. L. Messinge, *Chem Mater*. **2010**, *22*, 2061–2068. **DOI:**10.1021/cm903315u

17. D. Liu, Y. Yan, H. Zhou, *J Am Ceram Soc*. **2007**, *90*, 1323–1326. **DOI:**10.1111/j.1551-2916.2007.01525.x
18. K. Watari, B. Brahmaroutu, G. L. Messing, S. Trolier-McKinstry, S. C. Cheng. *J Mater Res*. **2000**, *15*, 846 –849. **DOI:**10.1557/JMR.2000.0121
19. Y. Saito, H. Takao. *Jpn J Appl Phys.* **2006**, *45*, 7377–7381. **DOI:**10.1143/JJAP.45.7377
20. D. Hu, H. Ma, Y. Tanaka, L. Zhao, Q. Feng. *Chem Mater*. **2015**, *27,* 4983–4994. **DOI:**10.1021/acs.chemmater.5b01368
21. P. Zhang, T. Ochi, M. Fujitsuka,Y. Kobori, T. Maima, T. Tachikowa. *Angew Chem Int Ed.* **2017**, *56*, 5299–5303. **DOI:**10.1002/anie.201702223
22. J. F. Cao, Y. X. Ji, *Chin Phys B*. **2014**, *23*, 128104. **DOI:**10.1088/1674-1056/23/12/128104
23. J. Cao, X. Huang, Y. Liu, J. Wu, Y. Ji, *Mater Res Express*. **2016**, *3*, 115903. **DOI:**10.1088/2053-1591/3/11/115903
24. R. Asiaie, W. D. Zhu, S. A. Akbar, P. K. Dutta, *Chem Mater*. **1996**, *8*, 226–234. **DOI:**10.1021/cm950327c
25. H. I. Hsiang, F. S. Yen, *Jpn J Appl Phys*. **1993**, *32*, 5029–5035. **DOI:**10.1143/JJAP.32.5029
26. V. Kalyani, B. S. Vasile, A. Ianculescu, M. T. Buscaglia, V. Buscaglia, P. Nanni, *Cryst Growth Des*. **2012**, *12*, 4450–4456. **DOI:**10.1021/cg300614f
27. T. Jardiel, A. C. Caballero, J. F. Fernández, M. Villegas, *J Eur Ceram Soc*. **2006**, *26*, 2823–2826. **DOI:**10.1016/j.jeurceramsoc.2005.05.003

Povzetek

$Bi_4Ti_3O_{12}$ delce z obliko, podobno ploščicam smo sintetizirali s pomočjo enostopenjske metode v staljeni soli iz nanodelcev Bi_2O_3 in TiO_2 pri 800 °C. Natančno smo raziskali reakcijske pogoje, ki vplivajo na kristalno strukturo in morfologijo. Razlike med različnimi delci $Bi_4Ti_3O_{12}$ smo preučili z vidika faznega prehoda iz feroelektrične v paraelektrično modifikacijo in fotokatalitske učinkovitosti za razgradnjo Rhodamina B pri svetlobnem obsevanju UV-A. V nadaljevanju smo tako pripravljene $Bi_4Ti_3O_{12}$ ploščice uporabili kot izhodiščne delce za pripravo $SrTiO_3$ ploščic s topokemijsko pretvorbo pod hidrotermalnimi pogoji. Določili smo značilnosti $Bi_4Ti_3O_{12}$ ploščic in reakcijske pogoje, pri katerih so $SrTiO_3$ delci ohranili obliko izhodiščnih ploščic $Bi_4Ti_3O_{12}$.